

Direct Detection of Nitroxyl in Aqueous Solution Using a Tripodal Copper(II) BODIPY Complex

Joel Rosenthal and Stephen J. Lippard*

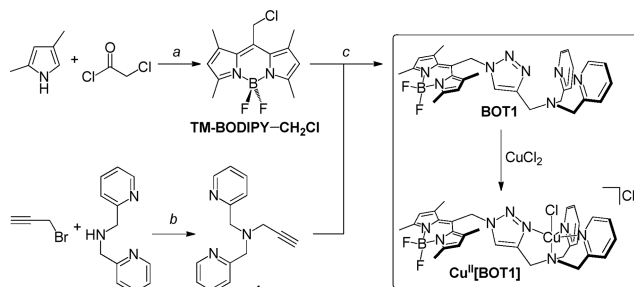
Department of Chemistry, Massachusetts Institute of Technology, 77 Massachusetts Avenue, Cambridge, Massachusetts 02139

Received October 27, 2009; E-mail: lippard@mit.edu

Nitric oxide (NO) mediates both physiological and pathological processes.^{1,2} In addition to cardiovascular signaling, NO has been invoked to play a neurochemical role in learning and memory, and it is a powerful necrotic agent wielded by macrophages of the immune system. Whereas considerable effort has been invested to develop metal-based^{3–5} and other^{6,7} probes for detecting nitric oxide, there has been significantly less progress in the synthesis of platforms capable of detecting other reactive nitrogen species (RNS).⁸ Of the nitrogen oxides relevant to biology, nitroxyl (HNO), the one-electron reduced, protonated analogue of nitric oxide,⁹ is among the least thoroughly investigated.¹⁰ Interest in nitroxyl has grown with the accumulation of evidence that HNO, which has a pK_a of 11.4 and exists primarily in the protonated form under physiological conditions,⁹ displays important biological roles with potential pharmacological applications distinct from those of nitric oxide.^{11–13} For example, HNO reacts directly with thiols,¹⁴ is resistant to scavenging by superoxide,¹⁵ and can activate voltage-dependent K^+ channels in mammalian vascular systems.^{16,17} Moreover, biochemical studies suggest that HNO can be formed directly from nitric oxide synthase under appropriate conditions^{10,18} and that NO and HNO may be able to interconvert in the presence of superoxide dismutase (SOD).¹⁹ Despite accumulating evidence of the biological importance of HNO, studies have been hampered by the lack of a biologically compatible probe for the molecule. Only recently have chemical systems capable of discerning HNO from NO been reported, but these constructs are not suitable for work with biological samples.^{20,21}

Properties required for selective nitroxyl detection using fluorescence methods under physiologically relevant conditions include selectivity over other RNS and downstream NO oxidation products, compatibility with living biological samples, water solubility, and membrane permeability. Additionally, incorporation of a signaling moiety with relatively long-wavelength absorption and emission properties is needed to avoid unintended cellular damage by high-energy radiation and to minimize innate biological autofluorescence. BOT1 (Scheme 1) juxtaposes a BODIPY reporter site, which has optical properties that are well suited for cellular imaging experiments,²² with a tripodal dipicolylamine-appended receptor via a triazole bridge. The tripodal metal-binding site of BOT1 comprises a tertiary nitrogen bearing two 2-pyridylmethyl substituents. The third arm of the tripod is afforded by the triazole formed upon coupling of an alkyl azide with a terminal alkyne.²³ Accordingly, the triazole arm completes the tripodal coordination environment engendered by the *N*-(triazolylmethyl)-*N,N*-dipicolyl framework while simultaneously providing a rigid spacer between the BODIPY reporter and chelating ligand. This design serves to minimize the distance between fluorophore and metal binding site, thereby assuring strong fluorescence quenching in the probe off-state. The triazole arm was installed by the copper(I)-mediated click-coupling

Scheme 1. Synthesis of BODIPY-Triazole 1 (BOT1)^a



^a (a) 1. O₂, 2. NEt₃, 3. BF₃, OEt₂; (b) K₂CO₃; (c) NaN₃, CuI, sodium ascorbate, DMSO/H₂O.

of alkyne **1** with the azide produced upon in situ displacement of Cl[−] from TM-BODIPY-CH₂Cl by NaN₃.

The photophysical properties of BOT1 were assessed under simulated physiological conditions (50 mM PIPES, 100 mM KCl, pH = 7.0). The probe displays optical properties typical of a BODIPY chromophore, with an absorption band in the visible region centered at 518 nm ($\epsilon = 30\,900 \pm 960 \text{ M}^{-1} \text{ cm}^{-1}$). Excitation into these bands produces an emission profile with a maximum at 526 nm and $\Phi_f = 0.12$ (Figure 1). Upon addition of 1 equiv of CuCl₂ to a solution of BOT1, the fluorescence intensity decreased by ~12-fold ($\Phi_f = 0.01$) and the lifetime by 30-fold (Figure S1, Supporting Information), which we attribute to photoinduced electron transfer (PET) from the BODIPY singlet excited state to the bound Cu²⁺ ion. The positive ion electrospray mass spectrum of this species displayed a peak with $m/z = 638.3$, which corresponds to that of [Cu^{II}(BOT1)Cl]⁺ (calcd $m/z = 638.2$) (Figure S2). Titration of BOT1 with CuCl₂ produced the series of emission changes displayed in Figure S3, with an apparent dissociation constant of $K_d = 3.0 \pm 0.1 \mu\text{M}$ (Figure S3), as calculated by a Benesi–Hildebrand analysis. Photophysical data recorded for BOT1 and Cu^{II}[BOT1] are available (Table S1). Analytically pure [Cu(BOT1)Cl]·acetone has been obtained.

Treatment of a 1 μM solution of Cu^{II}[BOT1] with 1000 equiv of cysteine restored the emission to that of uncomplexed BOT1, owing to reduction of the paramagnetic Cu²⁺ ion. The positive ion electrospray mass spectrum of this reduced species showed a peak with $m/z = 604.3$, which corresponds to the cationic [Cu^I(BOT1)]⁺ complex (calcd $m/z = 604.0$) (Figure S4). A solution of Cu^{II}[BOT1] in buffered aqueous solution was treated with excess Angeli's salt, which generates an equimolar ratio of nitroxyl (HNO) and nitrite under physiological conditions.²⁴ A 4.3 \pm 0.6-fold increase in emission was observed, demonstrating fast HNO detection with significant turn-on under physiologically relevant conditions (Figure 1). Emission turn-on was visualized using as little as 50 μM Angeli's salt. Cu^{II}[BOT1] displayed a negligible change in emission when treated with a 1000-fold excess of NaNO₂, indicating that

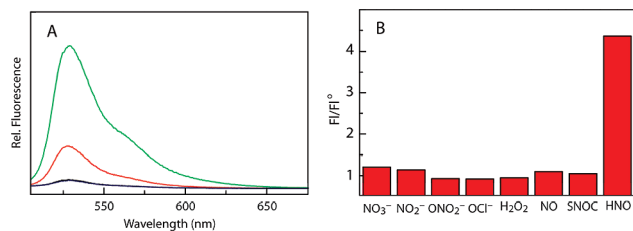


Figure 1. (A) Fluorescence spectrum of 3 μM BOT1 ($\lambda_{\text{exc}} = 450$ nm) in 50 mM PIPES buffer and 100 mM KCl (pH 7, 25 °C) (green) and spectral changes after addition of 2 equiv of CuCl_2 to generate $\text{Cu}^{\text{II}}[\text{BOT1}]$ (blue) and subsequent addition of 1000 equiv of Angeli's salt (red). (B) Fluorescence responses of 3 μM $\text{Cu}^{\text{II}}[\text{BOT1}]$ to various RNS and ROS (1.9 mM NO, 3.0 mM for all other RNS/ROS). Spectra were acquired in 50 mM PIPES and 100 mM KCl, pH = 7, and all data were obtained after incubation with the appropriate RNS/ROS at 25 °C for 1 h. Collected emission was integrated between 475 and 675 nm ($\lambda_{\text{exc}} = 450$ nm).

the turn-on response induced by Angeli's salt is due to HNO production and not the NO_2^- side product. HNO reacts with SODCu^{II} to generate NO and reduced SODCu^{I} .¹⁹ A similar reaction appears to occur with $\text{Cu}^{\text{II}}[\text{BOT1}]$, because treatment of the complex with Angeli's salt results in production of NO(g), as observed by EI-MS (Figure S5), concomitant with reduction of the paramagnetic Cu^{2+} complex to give the same $[\text{Cu}(\text{BOT1})]^+$ species observed by ESI-MS that is obtained upon reduction with cysteine (Figure S4). EPR spectroscopy provides further evidence for reduction of the paramagnetic $\text{Cu}^{\text{II}}[\text{BOT1}]$ complex by HNO (Figure S6). The emission response for $\text{Cu}^{\text{II}}[\text{BOT1}]$ is highly specific for HNO over other reactive species present in the biological milieu. Apart from NO_2^- , other RNS and reactive oxygen species (ROS), including NO, NO_3^- , ONOO^- , H_2O_2 , and OCl^- , failed to induce significant emission enhancement of the $\text{Cu}^{\text{II}}[\text{BOT1}]$ complex (Figure 1B). The negligible emission enhancement observed upon treatment of $\text{Cu}^{\text{II}}[\text{BOT1}]$ with saturated solutions of buffered NO is especially noteworthy and makes this system potentially valuable for studying the proposed disparate roles of NO and HNO in biology.

We next assessed the ability of $\text{Cu}^{\text{II}}[\text{BOT1}]$ to operate in live cells. HeLa cells were incubated with 1 μM $\text{Cu}^{\text{II}}[\text{BOT1}]$ (1 h, 37 °C). Under these conditions, cells show only faint intracellular fluorescence (Figure 2A). Addition of 200 μM Angeli's salt increased the observed intracellular red fluorescence over the course of 10 min, consistent with an HNO-induced emission response. No change in emission intensity was observed for the same time period for cultures to which Angeli's salt was not added (Figure S7). Moreover, treatment of HeLa cells preincubated for 30–90 min with $\text{Cu}^{\text{II}}[\text{BOT1}]$ with the NO donor diethylamine NONOate (200 μM) did not enhance the observed fluorescence (Figure S8). Addition of exogenous cysteine (200 μM) to cells pretreated with $\text{Cu}^{\text{II}}[\text{BOT1}]$ induced a rapid increase in emission (Figure S9), consistent with reduction to Cu^{I} . In related work, ascorbate was applied as an external reductant to image labile pools of copper.²⁵ The lack of a substantial fluorescent signal following addition of $\text{Cu}^{\text{II}}[\text{BOT1}]$ to cells assures that normal levels of intracellular cysteine and other thiols are insufficient to produce the fluorescent response that we observe for HNO.

$\text{Cu}^{\text{II}}[\text{BOT1}]$ is the first fluorescent molecular probe with visible excitation and emission profiles for detecting HNO in living biological samples. It features excellent selectivity for HNO over other biologically relevant RNS, including NO. The development of cell-trappable, longer-wavelength emission $\text{Cu}^{\text{II}}[\text{BOT1}]$ homologues aimed at unraveling the biology of HNO in living systems is in progress.

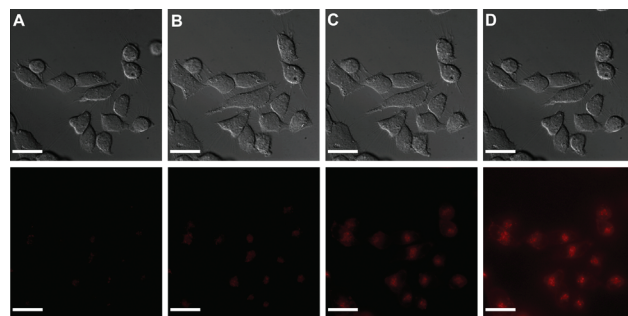


Figure 2. HNO-induced fluorescence response in HeLa cells (A) stained with 1 μM $\text{Cu}^{\text{II}}[\text{BOT1}]$ and (B) 1 min, (C) 5 min, and (D) 10 min after treatment with Angeli's salt (200 μM). (Top) DIC images and (bottom) fluorescence images. Scale bar, 25 μm .

Acknowledgment. We thank Dr. Daniel A. Lutterman for assistance with fluorescence lifetime measurements and Yogesh Surendranath for help with EI-MS. J.R. acknowledges postdoctoral fellowship support from the NIH (F32 GM080060-02). This work was supported by NSF grant CHE-0611944.

Supporting Information Available: Experimental procedures, characterization data, Table S1, and Figures S1–S9. This material is available free of charge via the Internet at <http://pubs.acs.org>.

References

- (1) Murad, F. *Biosci. Rep.* **1999**, *19*, 133–154.
- (2) Moncada, S.; Palmer, R. M. J.; Higgs, E. A. *Pharmacol. Rev.* **1991**, *43*, 109–142.
- (3) Lim, M. H.; Lippard, S. J. *Acc. Chem. Res.* **2006**, *40*, 41–51.
- (4) Lim, M. H.; Wong, B. A.; Pitcock, W. H., Jr.; Mokshagundam, D.; Baik, M. H.; Lippard, S. J. *J. Am. Chem. Soc.* **2006**, *128*, 14364–14373.
- (5) Lim, M. H.; Xu, D.; Lippard, S. J. *Nat. Chem. Biol.* **2006**, *2*, 375–380.
- (6) Kojima, H.; Nakatsubo, N.; Kikuchi, K.; Kawahara, S.; Kirino, Y.; Nagoshi, H.; Hirata, Y.; Nagano, T. *Anal. Chem.* **1998**, *70*, 2446–2453.
- (7) Kim, J.-H.; Heller, D. A.; Jin, H.; Barone, P. W.; Song, C.; Zhang, J.; Trudel, L. J.; Wogan, G. N.; Tannenbaum, S. R.; Strano, M. S. *Nat. Chem.* **2009**, *1*, 473–481.
- (8) Hughes, M. N. *Biochim. Biophys. Acta* **1999**, *1411*, 263–272.
- (9) Irvine, J. C.; Ritchie, R. H.; Favaloro, J. L.; Andrews, K. L.; Widdop, R. E.; Kemp-Harper, B. K. *Trends Pharmacol. Sci.* **2008**, *29*, 601–608.
- (10) Fukuto, J. M.; Dutton, A. S.; Houk, K. N. *ChemBioChem* **2005**, *6*, 612–619.
- (11) Miranda, K. M.; Paolucci, N.; Katori, T.; Thomas, D. D.; Ford, E.; Bartberger, M. D.; Espey, M. G.; Kass, D. A.; Feelisch, M.; Fukuto, J. M.; Wink, D. A. *Proc. Natl. Acad. Sci. U.S.A.* **2003**, *100*, 9196–9201.
- (12) Wink, D. A.; Miranda, K. M.; Katori, T.; Mancardi, D.; Thomas, D. D.; Ridnour, L.; Espey, M. G.; Feelisch, M.; Colton, C. A.; Fukuto, J. M.; Pagliaro, P.; Kass, D. A.; Paolucci, N. *Am. J. Physiol. Heart Circ. Physiol.* **2003**, *285*, H2264–2276.
- (13) Ma, X. L.; Gao, F.; Liu, G.-L.; Lopez, B. L.; Christopher, T. A.; Fukuto, J. M.; Wink, D. A.; Feelisch, M. *Proc. Natl. Acad. Sci. U.S.A.* **1999**, *96*, 14617–14622.
- (14) Fukuto, J. M.; Bartberger, M. D.; Dutton, A. S.; Paolucci, N.; Wink, D. A.; Houk, K. N. *Chem. Res. Toxicol.* **2005**, *18*, 790–801.
- (15) Espey, M. G.; Miranda, K. M.; Thomas, D. D.; Wink, D. A. *Free Radical Biol. Med.* **2002**, *33*, 827–834.
- (16) Irvine, J. C.; Favaloro, J. L.; Kemp-Harper, B. K. *Hypertension* **2003**, *41*, 1301–1307.
- (17) Irvine, J. C.; Favaloro, J. L.; Widdop, R. E.; Kemp-Harper, B. K. *Hypertension* **2007**, *49*, 885–892.
- (18) Hobbs, A. J.; Fukuto, J. M.; Ignarro, L. J. *Proc. Natl. Acad. Sci. U.S.A.* **1994**, *91*, 10992–10996.
- (19) Murphy, M. E.; Sies, H. *Proc. Natl. Acad. Sci. U.S.A.* **1991**, *88*, 10860–10864.
- (20) Marti, M. A.; Bari, S. E.; Estrin, D. A.; Doctorovich, F. *J. Am. Chem. Soc.* **2005**, *127*, 4680–4684.
- (21) Tennyson, A. G.; Do, L.; Smith, R. C.; Lippard, S. J. *Polyhedron* **2007**, *26*, 4625–4630.
- (22) Loudet, A.; Burgess, K. *Chem. Rev.* **2007**, *107*, 4891–4932.
- (23) Huang, S.; Clark, R. J.; Zhu, L. *Org. Lett.* **2007**, *9*, 4999–5002.
- (24) Liochev, S. I.; Fridovich, I. *Free Radical Biol. Med.* **2003**, *34*, 1399–1404.
- (25) Domaille, D. W.; Zeng, L.; Chang, C. J. *J. Am. Chem. Soc.* **2010**, *132*, 1194–1195.

JA909148V